An OpenFOAM-based electro-hydrodynamical model

Ivo Roghair[1], Dirk van den Ende[1], Frieder Mugele[1]

[1] *Department of Science and Technology, University of Twente, Enschede, The Netherlands*

Keywords: modelling, volume of fluid, openfoam, electrohydrodynamics

Abstract

In this work we present an OpenFOAM-based electro-hydrodynamics model. We have incorporated Gauss's Law and a free charge transport equation in an existing Volume-Of-Fluid model delivered with OpenFOAM. With the model it is possible to simulate the interaction of a fluid-fluid interface with an electric field, using perfect dielectric liquids as well as conductive liquids. Our implementation is validated using two approaches; first off, we simulate two vertically stacked liquids subjected to an electric field. The potential distribution is compared to the analytical result and a good comparison is found, using either a combination of two perfect dielectric liquids and a dielectric and a conductive liquid. For the latter case, we also find a good agreement with the theoretical relation for the surface charges. Secondly, we have simulated an artificial charge bump in a conductive liquid, and verify the charge transport equation by comparing the decay of the charge over time. Again, a good agreement with theory is found. Finally, we present a test case where we break up a droplet in an electric field. With that, we have shown to have a reliable EHD implementation in the OpenFOAM framework. For our future goal to simulate electrowetting phenomena, we require the electric field distribution in a coupled solid phase as well; we will use the current EHD model and extend it to a multi-region solver to include those effects.

Introduction

Electrowetting refers to an electrostatically induced reduction in the contact angle of an electrically conductive liquid droplet in an ambient dielectric fluid, placed on a solid substrate. The phenomenon has recently attracted increasingly more attention, especially in the field of microfluidics (Mugele & Baret (2005)). When applied properly, this phenomenon allows to accurately manipulate tiny amounts of liquid, e.g. the transportation, splitting, merging, or mixing of droplets, without the need for mechanical parts, which may degrade over time. As such, this technology has found its way to applications such as lab-on-a-chip (Cho et al., 2003 and Srinivasan et al., 2004), optofluidics (Berge & Peseux, 2000) and display technology (Hayes & Feenstra (2003)).

To guarantee reliable devices for these applications, many tedious experiments need to be performed. The availability of a numerical model to simulate electrowetting phenomena can guide the design of the, often complex, geometries involved.

Nowadays, several commercial software packages, allowing for a simultaneous simulation of electrostatics and hydrodynamics, are available. These packages can be very user friendly, are reasonably accurate and often allow for a freely designed geometry. However, due to the commercial nature of these programs, features such as parallel computation often involve additional payments. Without access to the source code the underlying numerical schemes cannot be modified (or even be reviewed), and extending the models with user-defined functionality is limited.

Open-source alternatives do exist, such as the well documented and validated Gerris Flow Solver, which has been developed over the past 10 years (Popinet (2003)), and also contains an electro-hydrodynamics module (López-Herrera (2011)).

In this work, we use the widely used open-source package OpenFOAM and extend it with an electro-hydrodynamical model. We have chosen to use OpenFOAM by its large community, broad range of available additional tools and relative ease to set up complex geometries.

Note that electrowetting is essentially a subset of the field of electro-hydrodynamics, and in this work we describe the fluid-fluid part of the model. Eventually, our goal is to include multiple regions (i.e. coupled solid and fluid regions), to be able to simulate electrowetting processes in full detail; the electric field distribution in the solid substrate is very important to the behavior of the fluid-fluid interface on the substrate and hence they need to be resolved in a coupled manner.

This paper continues with an outline of the used numerical schemes, followed by a number of validation cases. We then show simulation results of a droplet breaking up due to an externally applied electric field, and wrap up with our main conclusions.

Nomenclature

$\vec{E}$	electric field (V/m)
F	force (N)
g	gravitational constant (ms^{-2})
p	pressure (Nm^{-2})
t	time (s)
$\overset{\leftrightarrow}{T}$	maxwell stress tensor (Nm^{-2})

$\vec{u}$ velocity (ms^{-1})

Greek letters
α   phase fraction (-)
μ   viscosity (Pas)
ρ   density (kgm^{-3})
γ   surface tension coefficient (Nm^{-1})
σ   Surface charge (Cm^{-2})
κ   electric conductivity (Sm^{-1})
ε   electric permittivity (Fm^{-1})
φ   electric potential (V)

Subsripts
E   electric
γ   surface tension

Numerical Scheme

OpenFOAM is an open-source software package capable of numerically solving a wide range of CFD-related problems, e.g. fluid flow through complex domains, multiphase flows or fluid flows combined with other transport processes such as heat transfer. Though its documentation and validation cases are limited, it is backed by a huge community and a fair number of industrial users. Thanks to its open nature, we are able to incorporate the electrostatic field equations and the interaction of the electric field with the fluid-fluid interface into the existing framework. We are using the source code of 'interFoam' as a base model. While the basics of this model are described below, an extensive evaluation and verification of this multiphase-flow solver is given in the recent work of Deshpande et al. (2012) and references therein.

Fluid flow
The fluid flow field is solved via the incompressible Navier-Stokes equations, given in Eq. (1) and (2).

$$\rho \left(\frac{\partial \vec{u}}{\partial t} + \vec{u} \cdot \nabla \vec{u} \right) = \qquad (1)$$
$$-\nabla p + \nabla \cdot \left[\mu \left(\nabla \vec{u} + \nabla \vec{v}^T \right) \right] + \rho \vec{g} + \vec{F}_\gamma + \vec{F}_E$$

$$\nabla \cdot \vec{u} = 0 \qquad (2)$$

The additional terms $\vec{F}_\gamma$ and $\vec{F}_E$ represent the forces due to surface tension and the electric field, respectively.
The current multi-fluid method incorporated in OpenFOAM is based on the widely used volume-of-fluid (VOF) method (Hirt & Nichols, 1981), allowing to simulate fluid-fluid flows with dynamic interfaces including surface tension forces. Its advantages are intrinsic volume conservation and possibility of topological changes, e.g. break-up or merging of several entities, but the method lacks a sharp interface as seen in other methods, e.g. Front-Tracking (Unverdi & Tryggvason (1991), Dijkhuizen et al. (2010)) or Level-Set (Osher & Fedkiw, 2001). To prevent smearing of the phase fraction beyond reason, OpenFOAM makes use of a compression algorithm. Deshpande et al. (2012) provides a detailed description of the internal workings of the

compression algorithm, but it can be thought of as a inverse diffusion method to increase the gradient of the phase fraction at the interface position.
The VOF method describes the fluids and the interfaces by accounting for a phase fraction parameter α. Each time step, the phase fraction is advected with the fluid flow via Eq. (3)

$$\frac{\partial \alpha}{\partial t} + \nabla \cdot (\alpha \vec{u}) = 0 \qquad (3)$$

In the transition region (0<α<1), the density and viscosity are obtained via weighted arithmetic averaging with the phase fraction:

$$\rho = \rho_1 \alpha + \rho_2 (1 - \alpha) \qquad (4)$$
$$\mu = \mu_1 \alpha + \mu_2 (1 - \alpha) \qquad (5)$$

The surface tension force $\vec{F}_\gamma$ is obtained using the continuum surface force (CSF) model due to Brackbill et al. (1992) (see Deshpande et al. (2012) for details).

Electric equations
To account for the electrostatic field, we solve Gauss's law which relates the electrostatic field $\vec{E} = -\nabla \phi$ with free electric charges in the domain:

$$\nabla \cdot (\varepsilon \nabla \phi) = -\rho_E \qquad (6)$$

in which ε denotes the electric permittivity, ϕ is the electric potential and ρ_E is the electric charge density. The latter quantity is advected with the fluid flow and conducted according to the fluid conductivity using the following transport equation:

$$\frac{\partial \rho_E}{\partial t} + \nabla \cdot (\rho_E \vec{u}) = \nabla \cdot (\kappa \nabla \phi) \qquad (7)$$

Here, κ denotes the conductivity of the fluid. In the transition region, they are obtained via harmonic averaging weighted with the phase fraction:

$$\frac{1}{\kappa} = \frac{\alpha}{\kappa_1} + \frac{1 - \alpha}{\kappa_2} \qquad (8)$$

$$\frac{1}{\varepsilon} = \frac{\alpha}{\varepsilon_1} + \frac{1 - \alpha}{\varepsilon_2} \qquad (9)$$

Finally, we couple the electrostatic field to the fluid-fluid interfaces via the Maxwell stress tensor in the fluid flow equations.

$$F_E = \nabla \cdot \vec{\vec{T}} \qquad (10)$$
$$\vec{\vec{T}} = \varepsilon \left(\vec{E}\vec{E} - \frac{|\vec{E}|^2}{2} \vec{I} \right) \qquad (11)$$

With these equations included, the model is able to solve both dielectric and fully conductive liquids, and any combination of the two.
The electric equations are solved on the same computational mesh as the fluid flow equations. We have also taken care that the dynamic meshing feature delivered

with interFoam is conserved, which allows to refine the mesh according to a user-defined criterium (typically near the interface). For each variable, boundary conditions can be set, such as Neumann (zero-flux), Dirichlet (fixed value), but also a contact angle for the fluid-fluid interface.

Results and Discussion

This section starts with a discussion of two validation cases, which were set up according to the description in López-Herrera et al. (2011). Then, a more applied example of a droplet breakup due to an electric field is examined following an example in Bjørklund (2009).

Validation: vertically stacked liquids

We have conducted several validation simulations to test our current implementation. First of all, the implementation of Gauss's Law is investigated using two vertically stacked liquids, where the bottom liquid is termed '1' and the top liquid is termed '2'. The top electrode is grounded and the bottom electrode was set to unit potential. The first system consists of two perfect dielectric liquids, the second system consists of a conductive liquid 1 and a dielectric liquid 2. Since we only test for the electric potential and free charges, other parameters (*viz.* density, viscosity, etc) are not required here. A summary of the electrical properties is given in Table 1.

	Dielectric-Dielectric	Dielectric-Conductive
$\varepsilon\varepsilon_0$ (1)	$1\cdot10^{-11}$ F/m	$1\cdot10^{-12}$ F/m
$\varepsilon\varepsilon_0$ (2)	$3\cdot10^{-11}$ F/m	$3\cdot10^{-12}$ F/m
κ (1)	0 S/m	0 S/m
κ (2)	0 S/m	10^{-3} S/m

Table 1: Electrophysical properties of the validation case with two vertically stacked liquids in an electric field. The bottom liquid is identified by 1, the top liquid by 2.

The simulations have been performed in a two-dimensional simulation (1 cell in the z-direction), with height 1 and width 0.1 (in OpenFOAM, a problem should be at least two-dimensional but we restrict the number of cells in the horizontal direction since the current investigation is one-dimensional). The resulting potential distribution through the liquids can be compared to the exact solutions (López-Herrera et al. (2011)). For two dielectric liquids:

$$\phi_1 = \frac{-2y + \beta}{1 + \beta} \qquad \phi_2 = \frac{\beta(1 - 2y)}{1 + \beta}$$

Where y is the vertical position and the ratio of permittivities is given by $\beta = \frac{\varepsilon_1}{\varepsilon_2}$.

For the dielectric-conductive simulation, the potential in the conductive medium is constant and full potential gradient is seen in the dielectric fluid:

$$\phi_1 = 1 \qquad \phi_2 = -2y + 1$$

The resulting simulated (markers) and exact (lines) profiles are shown in Figure 1, whereas the simulation snapshots are given in Figure 2. A good agreement with the analytical result is found and we can be assured that Gauss's Law has

been implemented correctly.
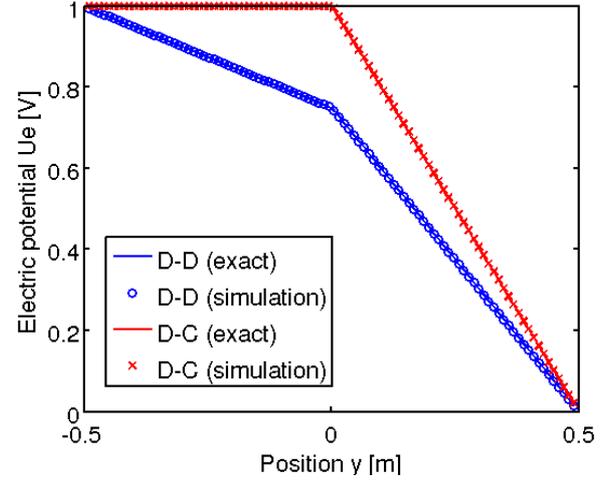
Figure 1: Electric potential distribution in two vertically stacked liquids, showing the result for two dielectric liquids (D-D) and a combination of a dielectric and a conductive liquid. The interface is located at y=0. The exact result (lines) is accurately reproduced by the simulations (markers).
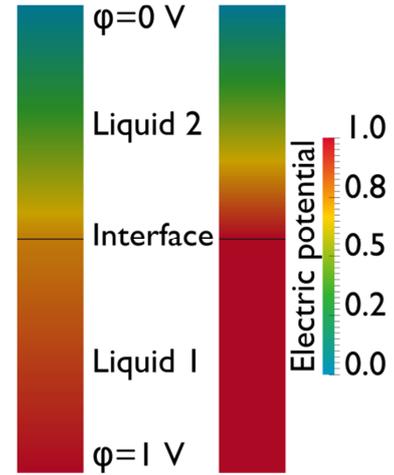
Figure 2: Snapshots of the simulation results.
Left: dielectric – dielectric
Right: dielectric (top) – conductive (bottom).

For the dielectric-conductive case, a free charge develops at the interface. In reality, the charge would be present at the interface (surface charge, σ), but in the simulations the free charges are represented by a charge density ρ_E. By volume integration of the free charges in the domain and dividing by the effective liquid-liquid interface yields a surface charge of σ = $2.01\cdot10^{-12}$ C/m^2, whereas one can obtain the surface charge via:

$$\sigma = \frac{\varepsilon_0(\varepsilon_2\kappa_1 - \varepsilon_1\kappa_2)}{\kappa_1 h_2 + \kappa_2 h_1}\phi = 2.00 \cdot 10^{-12}$$

where h_1 and h_2 are the heights of the layers.

Thus, the charge that emerges on the interface is predicted well too, provided that the volumetric charge density is collapsed onto the surface.

Validation: charge relaxation

In order to verify the charge transport equation, another test case following López-Herrera et al. (2011) has been set up. We consider a two-dimensional Gaussian charge bump centered in a square domain consisting of a single, conducting liquid with conductivity $\kappa = 1$ S/m and $\varepsilon = 2$ F/m. (see Figure 3).
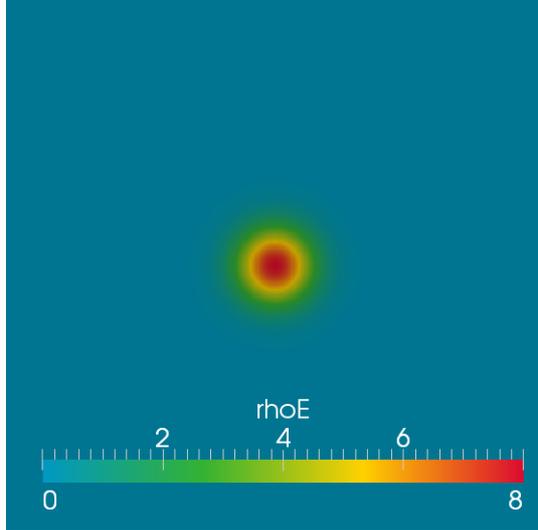
**Figure 3:** An initial Gaussian charge bump is centered in a square domain filled with a conducting medium.

The boundaries are fit with zero-gradient boundary conditions for the charge density and the electric potential. The initial charge density profile is set according to:

$$\rho_E(\vec{x}, t = 0) = \frac{e^{-r^2/2a^2}}{a\sqrt{2\pi}}$$

where $r^2 = x^2 + y^2$ and $a = 0.05$. The domain size was set to 1, and as time proceeds the charge bump decays exponentially following:

$$\rho_E(\vec{x}, t) = \rho_E(\vec{x}, t = 0)e^{-\kappa t/\varepsilon}$$

Figure 4 presents a comparison of the simulation results (markers) and analytical result (lines).
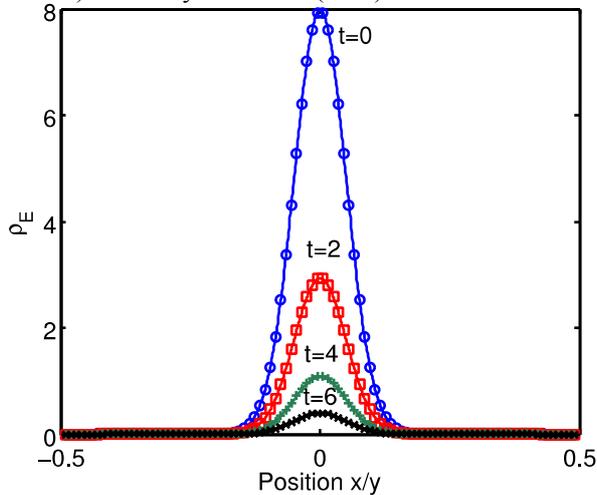
Figure 4: The charge density profile throughout the domain at different times. Markers indicate the simulation result, lines indicate the analytical relation.

In conclusion, we have validated our newly implemented equations in different ways and found a good correspondence with the analytical relations. Therefore, we can now put the model to the test and try a more realistic and dynamic application of the EHD code.

Case: Droplet break-up

Finally, we are showing an EHD case that includes the interaction of the electric field with the fluid-fluid interface. We will consider a droplet breaking up due to an alternating electric field following Bjørklund (2009).

The numerical setup consists of a two-dimensional domain of width 6*r* and height *12r* and a grid resolution of 0.1*r*. The left boundary is a symmetry boundary, and the other walls are solid walls with no-slip conditions. We use the symmetry condition to simulate a circular droplet (i.e. we initialise a semi-circle) vertically centered on the boundary, thus mimicking a full circle. The two liquids are perfect dielectrics with $\varepsilon_{ambient}/\varepsilon_{droplet}$=3/80. The density and viscosity of both liquids represent water, and the droplet radius is 0.1 mm. The surface tension coefficient was set to $\gamma = 0.01$ N/m. The top and bottom boundaries are used as electrodes, where the top is grounded and the bottom wall is set to an alternating potential with a frequency of 12.5 Hz at 12 kV. The settings are detailed in Figure 5.

To use time-dependent boundary conditions, we make use of a community-developed package called 'groovyBC'.
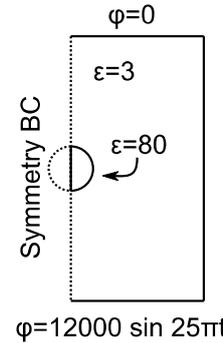
Figure 5: Numerical set-up for the droplet break-up case.

As the simulation starts, the electric field starts to pull on the interface. A number of snapshots are given in Figure 6. The droplet starts to stretch in the vertical direction and before the first cycle has ended, the droplet breaks up into three pieces. The result is very similar to that of Bjørklund (2009), with the exception that we find a small satellite droplet at the break-off point. We expect that this deviation is because Bjørklund (2009) used a level-set function to define the interface; the level-set method is known to have a sharp representation of the interface whereas the VOF method used in this work uses a diffuse interface technique.
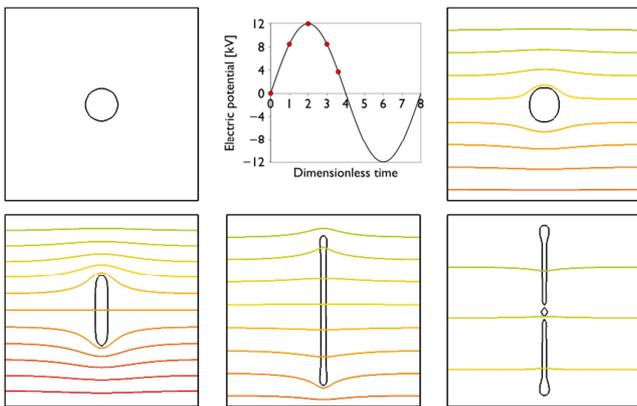
Figure 6: Droplet contours at different time steps of the simulation. The center image of the top row shows the position of the snapshots in the potential oscillation cycle. The bottom-right image shows the droplet contours at the moment of break-up, where a small satellite droplet emerges.

Conclusions and outlook

This work outlines an implementation of an electro-hydrodynamical model using the OpenFOAM framework. By solving for Gauss's Law and a charge density transport equation together with a volume-of-fluid multiphase flow code, we were able to set-up and solve several basic EHD problems. The simulation results have been verified with analytical solutions. Also, a more realistic use case has been presented, where a droplet centered in the domain breaks up due to interactions with the electric field.

In the future, we aim to develop a model to simulate electrowetting phenomena. For such problems, the electric field present in the solid dielectric substrate (preventing hydrolysis of the droplet) is essential. This field will alter the electrostatic field in the vicinity of the three-phase contact line and as such the whole electrowetting process. Therefore, it is essential to resolve the electrostatic field equations in the solid layer too. We have adopted a multi-region approach where the multi-phase fluid flow is considered in one region only, and the electric field equations are solved consistently in both regions.

Acknowledgements

References

Berge, B. & Perseux, J. Variable focal lens controlled by an external voltage: an application of electrowetting. European Physical Journal E, Vol. 3, 159-163 (2000).

Bjørklund, E. The level-set method applied to droplet dynamics in the presence of an electric field. Computers & Fluids, Vol 38, 358-369 (2009).

Brackbill, J.U., Kothe, D.B. & Zemach, C. A continuum method for modeling surface tension. Journal of computational physics, Vol. 100, 335-354 (1992).

Cho, S.K., Moon, H.J. & Kim, C.J. Creating, transporting, cutting, and merging liquid droplets by electrowetting-based actuation for digital microfluidic circuits. Journal of microelectromechanical systems, Vol. 12, 70-80 (2003).

Deshpande, S.S., Anumolu, L. & Trujillo, M.F. Evaluating the performance of the two-phase flow solver interFoam. Computational science & discovery, Vol. 5, 014016 (2012).

Dijkhuizen, W., Roghair, I., Van Sint Annaland, M. & Kuipers, J.A.M. DNS of gas bubbles behaviour using an improved 3D front tracking model-model development. Chemical Engineering Science, Vol. 65, 1427-1437 (2010).

López-Herrera, J.M., Popinet, S. & Herrada, M.A. A charge-conservative approach for simulating electrohydrodynamic two-phase flows using volume-of-fluid. Journal of Computational Physics, Vol 230, 1939-1955 (2011).

Hayes, R.A. and Feenstra, B.J. Video-speed electronic paper based on electrowetting, Nature, Vol. 425 (2003).

Hirt, C.W. & Nichols, B.D. Volume of fluid method for the dynamics of free boundaries. Journal of Computational Physics, Vol 39, 201-225 (1981).

Mugele, F. & Baret, J.-C. Electrowetting: from basics to applications , J. Phys.: Condens. Matter, Vol. 17 (2005) .

Popinet, S., Gerris: a tree-based adaptive solver for the incompressible Euler equations in complex geometries. Journal of computational physics, Vol. 190(2), 572-600 (2003).

Srinivasan V., Pamula V.K. & Fair R.B. An integrated digital microfluidic lab-on-a-chip for clinical diagnostics on human physiological fluids. Lab on a Chip, Vol. 4, 310-315 (2004).

Unverdi, S.O. & Tryggvason, G. A front tracking method for viscous, incompressible, multi-fluid flows. Journal of Computational Physics, Vol. 100, 25-37 (1992).